Draft version – February 1, 2008
Preprint typeset using LaTeX style emulateapj v. 10/09/06

DYNAMICAL FRICTION AND GALAXY MERGING TIMESCALES

Michael Boylan-Kolchin[1], Chung-Pei Ma[2], and Eliot Quataert[3]
Department of Astronomy, University of California, Berkeley, CA 94720
Draft version – February 1, 2008

ABSTRACT

The timescale for galaxies within merging dark matter halos to merge with each other is an important ingredient in galaxy formation models. Accurate estimates of merging timescales are required for predictions of astrophysical quantities such as black hole binary merger rates, the build-up of stellar mass in central galaxies, and the statistical properties of satellite galaxies within dark matter halos. In this paper, we study the merging timescales of extended dark matter halos using N-body simulations. We compare these results to standard estimates based on the Chandrasekhar theory of dynamical friction. We find that these standard predictions for merging timescales, which are often used in semi-analytic galaxy formation models, are systematically shorter than those found in simulations. The discrepancy is approximately a factor of 1.7 for $M_{\rm sat}/M_{\rm host} \approx 0.1$ and becomes larger for more disparate satellite-to-host mass ratios, reaching a factor of ~ 3.3 for $M_{\rm sat}/M_{\rm host} \approx 0.01$. Based on our simulations, we propose a new, easily implementable fitting formula that accurately predicts the timescale for an extended satellite to sink from the virial radius of a host halo down to the halo's center for a wide range of $M_{\rm sat}/M_{\rm host}$ and orbits. Including a central bulge in each galaxy changes the merging timescale by $\lesssim 10\%$. To highlight one concrete application of our results, we show that merging timescales often used in the literature overestimate the growth of stellar mass by satellite accretion by $\approx 40\%$, with the extra mass gained in low mass ratio mergers.

Subject headings: galaxies: evolution — galaxies: formation

1. INTRODUCTION

As originally formulated by Chandrasekhar (1943), the deceleration of an orbiting point mass "'satellite," due to dynamical friction on a uniform background mass distribution, is given by

$$\frac{d}{dt}\vec{v}_{\rm orb} = -4\pi G^2 \ln(\Lambda)\, M_{\rm sat}\, \rho_{\rm host}(< v_{\rm orb})\, \frac{\vec{v}_{\rm orb}}{v_{\rm orb}^3}\,, \qquad (1)$$

where $\rho_{\rm host}(< v_{\rm orb})$ is the density of background particles with velocities less than the orbital velocity $v_{\rm orb}$ of the satellite, $M_{\rm sat}$ is the mass of the satellite, and Λ is the usual Coulomb logarithm (e.g, Chandrasekhar 1943; White 1976).

Accurate estimates of the effects of dynamical friction and the timescale for an orbiting satellite to lose its energy and angular momentum to merge with a host are essential for many astrophysical problems. A thorough understanding of dynamical friction is particularly critical for semi-analytic models (SAMs) of galaxy formation. The growth of dark matter halos via mergers can be computed either analytically or via dissipationless cosmological simulations, but the growth of galaxies depends on their dynamical evolution within larger dark matter halos. As a result, dynamical friction (and tidal stripping, which determines $M_{\rm sat}$) provides a critical link between dark matter halo mergers and the galaxy mergers that determine, e.g., stellar masses, supermassive black hole masses, galaxy colors, and galaxy morphologies. Since it is computationally infeasible to simulate both dark matter on cosmological scales and baryonic physics relevant to galaxies, SAMs will remain an important tool for interpreting observations of galaxy formation and evolution for the foreseeable future.

There are, however, often significant uncertainties in directly applying equation (1) due to the approximate nature of the Chandrasekhar formula, and ambiguities in the appropriate value of the Coulomb logarithm and the definition of the satellite mass $M_{\rm sat}$ for extended objects (e.g., galaxies or dark matter halos). SAMs, for instance, typically use mild variations on the same basic formula for modeling the merger timescale $\tau_{\rm merge}$ induced by dynamical friction:

$$\frac{\tau_{\rm merge}}{\tau_{\rm dyn}} = 1.17\, \frac{f_{\rm df}\, \Theta_{\rm orb}}{\ln \Lambda}\, \frac{M_{\rm host}}{M_{\rm sat}} \qquad (2)$$

(e.g., eq. 7.26 of Binney & Tremaine 1987), where $\Theta_{\rm orb}$ contains information about the orbital energy and angular momentum, $f_{\rm df}$ is an adjustable parameter, and $\tau_{\rm dyn}$ is the dynamical timescale at the virial radius $r_{\rm vir}$ of the host halo, related to the circular velocity at $r_{\rm vir}$, $V_c(r_{\rm vir})$, by

$$\tau_{\rm dyn} \equiv \frac{r_{\rm vir}}{V_c(r_{\rm vir})} = \left(\frac{r_{\rm vir}^3}{G M_{\rm host}}\right)^{1/2}. \qquad (3)$$

Differences among different SAMs enter mainly in how each model treats $\ln\Lambda$, $\Theta_{\rm orb}$, and $f_{\rm df}$, as well as how $M_{\rm sat}$ is determined and when $\tau_{\rm merge}$ is determined (e.g., Kauffmann et al. 1993; Somerville & Primack 1999; Cole et al. 2000; Croton et al. 2006). Uncertainties in these parameters are reflected in equally large uncertainties in $\tau_{\rm merge}$.

The Coulomb logarithm, for example, should technically be expressed as $\frac{1}{2}\ln(1+\Lambda^2)$; using $\ln\Lambda$ is appropriate in the limit of large Λ (Binney & Tremaine 1987). The Coulomb logarithm represents the ratio of the largest and smallest impact parameters of field stars

[1] mrbk@berkeley.edu
[2] cpma@berkeley.edu
[3] eliot@astro.berkeley.edu

that contribute to small-angle scatterings of the satellite: $\Lambda = b_{\rm max}/b_{\rm min}$. This motivates a conventional choice for the Coulomb logarithm: $\Lambda = 1 + M_{\rm host}/M_{\rm sat}$, where $M_{\rm sat}$ is often taken to be the mass of the satellite when it enters the virial radius of the host halo of mass $M_{\rm host}$. Alternatively, the Coulomb logarithm can be taken to be a mass-independent constant (e.g., Cooray & Milosavljević 2005). When using equation (1) to model the full orbits of satellites, another approach is to assume that the Coulomb logarithm varies over the course of the orbit (e.g., Hashimoto et al. 2003; Zentner et al. 2005; Fellhauer & Lin 2007). These various prescriptions for the Coulomb logarithm can differ by a factor of 2-3.

In addition, it is known that $M_{\rm sat}$ cannot refer to just the bound mass for extended objects because tidally stripped material still in the vicinity of the satellite also contributes to dynamical friction (Fujii et al. 2006; Fellhauer & Lin 2007). The uncertainties in $\tau_{\rm merge}$ introduced by different prescriptions for $\ln\Lambda$ and $M_{\rm sat}$ are important for galaxy formation models because 50% changes in the timescale for galaxies to merge within dark matter halos could significantly change the predictions for galaxy growth via merging or cannibalism, black hole merger rates, and the evolution of satellite galaxies in groups and clusters.

Full dynamical models of the evolution of merging halos – complete with the physics of dynamical friction, tidal stripping, and gravitational shocking – have been created by a number of groups (e.g., Taylor & Babul 2001; Taffoni et al. 2003; Zentner et al. 2005; Gnedin 2003). These models, however, are based on approximate treatments of the underlying physical processes, and obtaining merging timescales would often require numerically integrating individual satellite orbits (Velazquez & White 1999). In this paper we take a different approach and instead compute merger timescales directly using numerical simulations. We focus on the range of satellite masses and orbital parameters that are relevant for dark matter halo mergers in hierarchical galaxy formation models. Our goal is to provide a fitting formula that is as simple as possible but that still accurately reflects the physics of dynamical friction and tidal stripping.

The remainder of this paper is organized as follows. Section 2 describes the numerical simulations we have performed. In Section 3, we investigate the merging timescales $\tau_{\rm merge}$ computed from our numerical simulations, propose a new fitting formula for $\tau_{\rm merge}$, and compare to previous results. Section 4 contains two sample applications of our proposed fitting formula: an estimate of the mass spectrum and orbital distribution of merging galaxies. Our results and conclusions, and their implications, are reviewed in Section 5. Throughout this paper, we use "virial" quantities that are defined relative to $200\rho_c$, where ρ_c is the critical density. When necessary, we assume a cosmology of $\Omega_m = 0.3$, $\Omega_\Lambda = 1 - \Omega_m = 0.7$, and $H_0 = 70\,{\rm km\,s^{-1}\,Mpc^{-1}}$.

2. SATELLITE DECAY FROM NUMERICAL SIMULATIONS

2.1. *Description of simulations and initial conditions*

We have performed a number of numerical simulations to test the agreement between merger timescales predicted by equation (2) and those derived directly from N-body simulations. Each of our simulations consists of a host Hernquist (1990) halo and a satellite Hernquist halo; the ratio of satellite to host mass and the initial orbital parameters of the satellite are varied from run to run. The host and satellite halos were constructed using $N_{\rm host} = 2\times10^5$ particles for the host and equal particle masses for the host and satellite particles, i.e., $N_{\rm sat} = (M_{\rm sat}/M_{\rm host})\,2\times10^5$. Each halo was constructed by sampling the full phase-space distribution function (under the assumptions of spherical symmetry and velocity isotropy) and was tested to be stable when evolved in isolation. In addition, two simulations included a (self-consistently constructed) Hernquist bulge in both the host and satellite to test the effects of baryonic components on merging timescales.

The numerical simulations were run using GADGET-2 (Springel 2005). Outputs were saved every 0.1 Gyr, or equivalently, $\approx 0.06\,\tau_{\rm dyn}$. To ensure that our simulations are not affected by numerical artifacts, we have performed several convergence runs with respect to both the particle number (up to 10^6 particles in the host halo) and the force softening ϵ (which is reduced by up to a factor of 5 from our fiducial value of $\epsilon = 10^{-3}\,r_{\rm vir}$). Because our simulations involve only gravity, the length, mass, and time scales can be rescaled for any host halo mass; for definiteness, however, we quote our results for host halos of total mass $M_{\rm host} = 10^{12}\,M_\odot$ and Hernquist scale length $a = 40$ kpc. Matching to a Navarro et al. (1997, hereafter NFW) profile with a virial mass equal to the Hernquist halo's total mass and an identical density at $r \ll a$, our standard host halo corresponds to an NFW halo with a concentration ≈ 8.5 (see, e.g., Springel et al. 2005a for more details on how to relate Hernquist and NFW halos). A comparison run using an NFW halo had a merging timescale within 5% of that from the corresponding run with a Hernquist halo.

In the absence of dynamical friction, the orbit of a test particle in a static spherical potential is entirely specified by its energy E and angular momentum J. An equivalent parametrization for bound orbits is to use the orbital circularity

$$\eta \equiv \frac{j}{j_c(E)}\,, \tag{4}$$

which is the specific angular momentum relative to the specific angular momentum of a circular orbit with the same energy [η is related to eccentricity e by $\eta = (1-e^2)^{1/2}$], and $r_c(E)$, which is the radius of a circular orbit with the same energy as the particle in question. Since dynamical friction dissipates energy, the orbit of a satellite galaxy in a host galaxy generally depends on its initial position $r(t=0)$ in addition to $E(t=0)$ and $J(t=0)$.

We explore a range of orbital circularity η, energy $r_c(E)$, and satellite-to-host mass ratios $M_{\rm sat}/M_{\rm host}$ in our simulations. A summary of the production runs and the resulting $\tau_{\rm merge}$ is presented in Table 1. The ranges of the parameters are chosen so that the satellites can plausibly undergo significant orbital evolution within a Hubble time (see Sec. 3.2 for more details). Systems with mass ratios $M_{\rm sat}/M_{\rm host}$ much smaller than 1:40 are therefore dynamically uninteresting and excluded.

2.2. *Defining timescales: angular momentum loss*

TABLE 1
List of Simulations

Run (1)	M_{sat}/M_{host} (2)	circularity η (3)	$r_c(E)/r_{vir}$ (4)	τ_{merge} (5)
3b	0.3	0.78	1.0	4.4
3d	0.3	1.00	1.0	6.9
5b	0.2	0.46	1.0	3.5
5c	0.2	0.65	1.0	4.5
5d	0.2	0.78	1.0	6.0
5e	0.2	1.00	1.0	9.5
10a	0.1	0.33	1.0	4.85
10a⋆	0.1	0.33	1.0	4.3
10b	0.1	0.46	1.0	6.0
10c	0.1	0.65	1.0	8.25
10c⋆	0.1	0.65	1.0	7.8
10d	0.1	0.78	1.0	10.75
14b	0.0707	0.46	1.0	9.0
14c	0.0707	0.65	1.0	12.5
20a	0.05	0.33	1.0	10.0
20b	0.05	0.46	1.0	11.0
20c	0.05	0.65	1.0	17.0
40b	0.025	0.46	1.0	22.0
40c	0.025	0.65	1.0	38.0
10a1	0.1	0.33	0.65	3.5
10a4	0.1	0.33	0.80	4.3
10b1	0.1	0.46	0.65	4.3
10b4	0.1	0.46	0.80	5.0
10c1	0.1	0.65	0.65	5.6
10c2	0.1	0.65	0.70	5.5
10c3	0.1	0.65	0.75	6.2
10c4	0.1	0.65	0.80	6.35
10c5	0.1	0.65	0.90	7.5

Note. — Description of columns:
(1) Name of simulation
(2) Ratio of initial satellite mass to initial host halo mass
(3) Initial orbital angular momentum, parametrized by circularity η
(4) Initial orbital energy, parametrized by $r_c(E)/r_{vir}$
(5) Dynamical friction merging time τ_{merge}, in Gyr, for a host with virial mass $M_{host} = 10^{12}\,M_\odot$, measured from the simulation as described in Sec. 2
(⋆ indicates run with baryonic component; see §2.3 for details)

The timescale for a satellite to merge with its host halo can be defined in a number of different ways. One common definition is to take a fiducial radius of the baryonic component assumed to reside at the center of the halo and assume that the satellite has merged when its separation from the host's center equals this radius. In this work, we instead consider a satellite merged when it has lost all of its specific angular momentum $j \equiv r\,v_t$ (relative to the host). In practice, this definition agrees with the more commonly-used one in most cases but also works well for situations in which the definition based on orbital separation can give undesired results. Consider highly eccentric orbits, in which the satellite can come very close to the center of the host while retaining significant orbital energy; satellites on these orbits often do not merge for multiple dynamical times following the first close encounter. The specific angular momentum of the satellite should, however, be a non-increasing function of time, so using $j(t)/j_0$ [where $j_0 = j(t = 0)$] is therefore our preferred definition for merging.

Fig. 1 shows the trajectories (top) and angular momentum decay (bottom) for three sets of live-satellite simulations starting from r_{vir}, with $M_{sat}/M_{host} = 0.025$, 0.05, and 0.10, for two different orbital circularities, $\eta = 0.46$ (solid curves) and $\eta = 0.65$ (dashed curves). For a given circularity, systems with more disparate masses merge much more slowly, as is expected from basic dynamical friction considerations. For a given mass ratio, the satellite on the more eccentric orbit (i.e. smaller η) loses angular momentum faster, resulting in a more rapid merger. The difference is non-negligible even for mass ratios as similar as 1:3. In this case, a satellite with $\eta = 0.78$ merges in approximately 4.4 Gyr while a satellite on a circular orbit takes over 50% longer – 6.9 Gyr – to merge (see last column of Table 1).

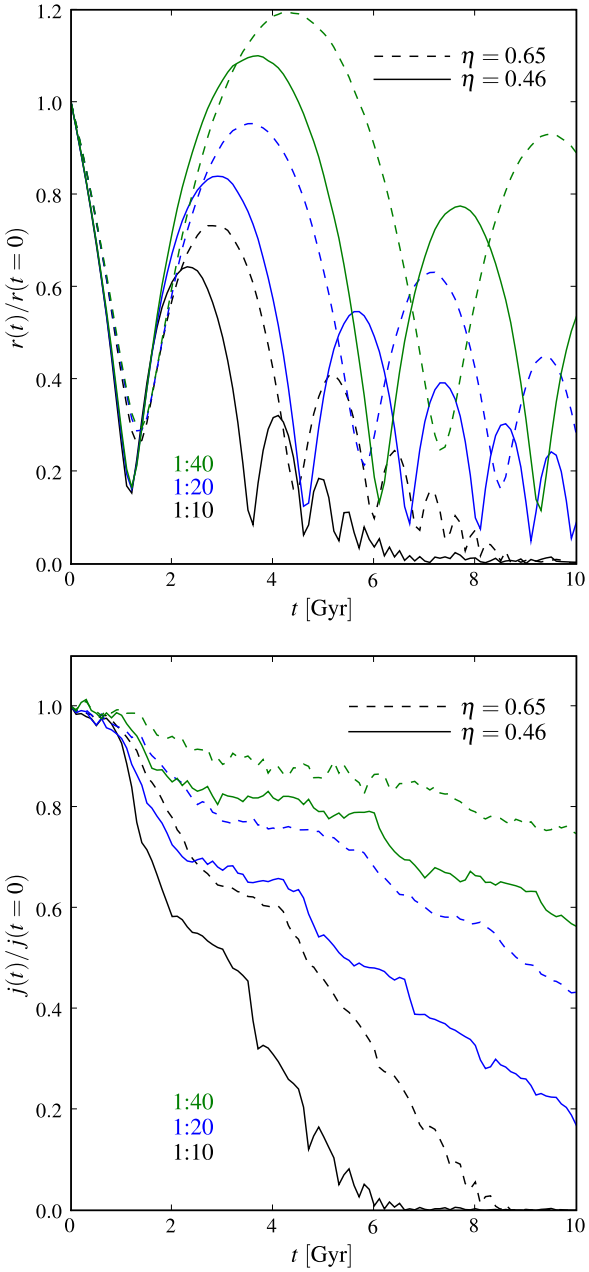

Fig. 1.— Top: Trajectories of satellites (i.e., separation between satellite and host centers) from six simulations with two different orbits – $\eta = 0.46$ (solid) and 0.65 (dashed) – and three different mass ratios: 1:10 (black), 1:20 (blue), and 1:40 (green). For all cases, satellites on more eccentric orbits (lower η) or with higher mass ratios merge more quickly. Bottom: angular momentum decay for the same satellites. The loss of angular momentum initially correlates well with pericentric passages but at later times $dj/dt \sim$ constant.

Fig. 1 highlights the angular momentum loss process. A comparison between the top and bottom panels shows

that the bulk of the angular momentum loss initially coincides with pericentric passages (e.g., at 1 and 4.5 Gyr for the 1:20 blue curves) and the accompanying tidal stripping and shocking (see also Boylan-Kolchin & Ma 2007). It is also interesting to note that while the angular momentum loss is initially somewhat impulsive, it later ($t \gtrsim 5$ Gyr) becomes nearly constant in time. Physically, the approximate constancy of $dj/dt \sim j/\tau_{\rm merge}(r)$ follows from the fact that the merger timescale at any radius is roughly linearly proportional to radius (see eq. [5] discussed below), as is j itself. It is also interesting to note that a satellite can continue to orbit for several giga-years even after its initial orbit has dipped within 5% of $r_{\rm vir}$ of the host (e.g., the 1:20 merger in Fig. 1). In fact, at the first pericentric pass within $\sim 5\%$ of $r_{\rm vir}$ (which occurs at $t \approx 6.5$ Gyr for $\eta = 0.46$), the satellite has only lost 60% of its initial angular momentum. Such satellites should *not* be considered merged even though they may pass very close to the center of the halo (within the radius at which a central galaxy might lie); our calculations show that these satellites will orbit for a significantly longer time before actually merging.

When the mass of the satellite is much less than the mass of the host, $\tau_{\rm merge}$ becomes prohibitively long to study with simulations, as numerical relaxation becomes an important effect. For these cases (only three runs: 20c, 40b, and 40c), we determine $\tau_{\rm merge}$ by linearly extrapolating $j(t)/j_0$. This tends to be a reasonable measure of the merging time as long as we extrapolate *after* the first two pericentric passages, where gravitational shocks and tidal stripping cause substantial changes in the angular momentum. After the first two pericentric passages, the angular momentum loss occurs at a roughly uniform rate.

2.3. *Effects of baryons*

Although the ratio of a galaxy's stellar mass to the virial mass of its dark matter halo does not exceed ≈ 0.1, it is conceivable that neglecting baryons could lead to significant errors in the predicted merging timescales. In particular, bulges in elliptical galaxies are significantly more dense than dark matter halos at the same physical scale, meaning that bulges are more resistant to disruption via tidal shocking. Thus, the expectation is that merger timescales would be shorter for full galaxy models than for dark matter halos alone.

In order to test the effects of the baryonic components of galaxies on merging timescales, we ran two additional simulations. Both simulations used $M_{\rm sat}/M_{\rm host} = 0.1$, but we included stellar bulges with $M_\star/M_{\rm dm} = 0.05$ in both the host and satellite for each simulation.[4] The effective radii of the bulges were chosen to be representative of those measured by Shen et al. (2003) from the Sloan Digital Sky Survey (York et al. 2000), $R_e \propto M_\star^{0.56}$, and the orbits of the two runs are identical to runs 10a and 10c.

In Fig. 2, we compare the angular momentum loss as a function of time for the runs without stars (solid curves) and with stars (dashed curves). Including stars does lead to faster mergers, as expected, but the difference in merging timescales is less than 10%, which is quite modest. When the satellite first enters the host's virial radius, the bulges contribute negligibly to dynamical friction drag because the baryons contribute $< 10\%$ to the system's total mass. At late stages in the merger, the bulges may be more important, as the dark matter halo is more efficiently stripped than the bulge. The satellites spend the vast majority of their time at large radii, however, so that the error introduced by ignoring baryons is small when considering the total time required to merge from the virial radius (see Fig. 2).

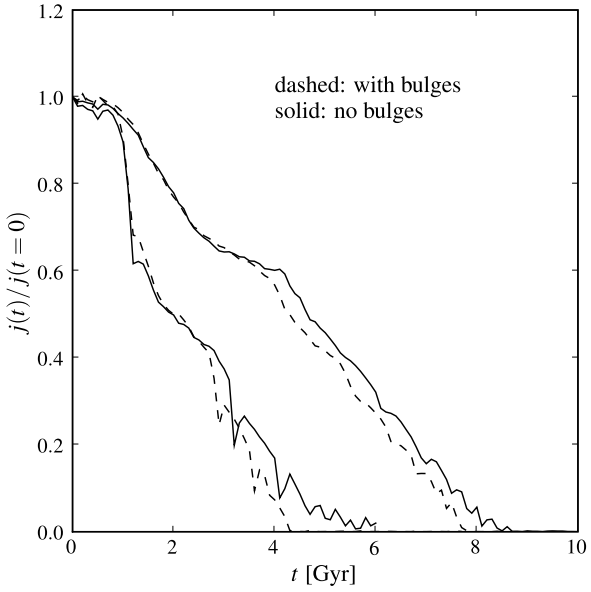

FIG. 2.— Effects of including baryonic components. The solid curves show the angular momentum loss for runs 10a (left; $\eta = 0.33$) and 10c (right; $\eta = 0.65$). The dashed curves show $j(t)/j_0$ for runs that have a stellar bulge (with $M_{\rm vir}/M_{\rm bulge} = 20$) in both the host and satellite but are otherwise identical. Including baryons leads to merger timescales that are $\lesssim 10\%$ shorter than those of the corresponding dark matter-only simulations.

3. COMPUTING MERGER TIMESCALES

In this section we provide a simple parameterization of the merging timescales determined from the numerical simulations discussed above. Comparisons between this new fitting formula and some commonly used ones in the literature are also presented (Sec 3.3).

3.1. *A fitting formula*

We fit the merger timescales from the simulations in Table 1 to a simple formula,

$$\frac{\tau_{\rm merge}}{\tau_{\rm dyn}} = A\,\frac{(M_{\rm host}/M_{\rm sat})^b}{\ln(1+M_{\rm host}/M_{\rm sat})}\exp\left[c\,\frac{j}{j_c(E)}\right]\left[\frac{r_c(E)}{r_{\rm vir}}\right]^d, \quad (5)$$

where the constants b, c, and d parameterize the dependence of the merger timescales on the host-to-satellite mass ratio $M_{\rm host}/M_{\rm sat}$, orbital circularity $\eta = j/j_c(E)$, and orbital energy $r_c(E)$, respectively. Both η and $r_c(E)$ are computed self-consistently using the Hernquist potential, *not* using the two-body approximation. To avoid ambiguities in the definition of satellite and host mass

[4] The bulge + dark matter halo systems for the initial conditions are set up self-consistently and are very stable over many dynamical times when evolved in isolation; see Boylan-Kolchin & Ma (2007) for details.

as a function of the location of the satellite (or time), we define the masses $M_{\rm host}$ and $M_{\rm sat}$ here as the *virial* masses of the host and the satellite when entering the host's virial radius. For the same reason, we use the specific angular momentum j rather than the full angular momentum J in computing the orbital properties of the satellites; since the circularity depends only on a ratio of angular momenta, this choice does not affect calculations of η. The dynamical time $\tau_{\rm dyn}$ is the dynamical time at the host's virial radius $r_{\rm vir}$ given by equation (3). Note that $\tau_{\rm dyn} = 0.1\,H^{-1}$ (where H is the Hubble constant) independent of the host halo mass; at $z = 0$, $\tau_{\rm dyn} = 1.4$ Gyr for $H = 70\,{\rm km\,s^{-1}\,Mpc^{-1}}$.

With the definitions above, we find that

$$A = 0.216\,, \quad b = 1.3\,, \quad c = 1.9\,, \quad d = 1.0 \qquad (6)$$

provide fits to the simulation results with a standard deviation of $< 7\%$ and a maximum deviation of 12.5%, a significant improvement over equation (2). To obtain the values in equation (6), we have chosen to fit to the parameter d separately from A, b, and c. For A, b, and c, we have fitted to $\tau_{\rm merge}$ from the subset of simulations in which the satellites begin at the virial radius of their host with an orbital energy $E = E_c(r_{\rm vir})$, i.e., with $r_c(E) = r_{\rm vir}$, and the fit is independent of d. To determine the value of d in equation (6), we use the series of simulations with $M_{\rm sat}/M_{\rm host} = 0.1$ and $r_c(E)/r_{\rm vir} = [0.65, 0.7, 0.75, 0.8, 0.9, 1.0]$ (all starting at $r_{\rm vir}$). Holding A, b, and c fixed, we investigate whether any single choice of d results in a consistently accurate prediction of the merging timescale.

The close agreement between the numerical simulations and the fits in equation (5) is illustrated by the circles in Fig. 3 and squares in Fig. 4. The two figures show the ratio of the timescale measured from each simulation, $\tau_{\rm merge}$(sim), to the timescale predicted by equation (5), $\tau_{\rm merge}$(fit), for a wide range of orbital energy ($0.65 \le r_c(E)/r_{\rm vir} \le 1.0$), orbital circularity ($0.33 \le \eta \le 1$), and satellite-to-host halo mass ($0.025 \le M_{\rm sat}/M_{\rm host} \le 0.3$). In addition, Fig. 3 shows that using $d = 1.0$ (circle symbols) in equation (5) results in good agreement between predicted and measured $\tau_{\rm merge}$, while the often used $d = 2.0$ (diamond symbols) results in a poor match, systematically underestimating $\tau_{\rm merge}$ (see §3.3.2 for more discussion). In Fig. 4, we also compare $\tau_{\rm merge}$(fit) to that predicted by a fiducial SAM, $\tau_{\rm merge}$(SAM); this is discussed in §3.3 below.

A further point of interest is that using $d \approx 1$ in Equation (5) also provides a significantly better fit than $d = 2$ when considering the merging timescale as a function of position along a given orbit. This suggests that equation (5) can be used for starting radii other than $r_{\rm vir}$, though its accuracy will certainly decline for $r \ll r_{\rm vir}$. This possibility is not explored in any more detail in this paper, however, and we restrict ourselves to starting radii of $r_{\rm vir}$.

3.2. *Range of validity*

We have chosen to simulate parameters that correspond to probable satellite orbits in a ΛCDM cosmology. The mass ratios we have considered – $0.025 \le M_{\rm sat}/M_{\rm host} \le 0.3$ – cover a reasonable range, as lower mass ratios are unlikely to merge within even multiple Hubble times, while mass ratios near unity merge on nearly a dynamical time. We note that Eqn. 5 does indeed tend toward $\tau_{\rm merge} \approx \tau_{\rm dyn}$ for $M_{\rm sat} = M_{\rm host}$ and $\eta \approx 0.5$; it therefore should give a reasonable approximation even for our untested regime of $M_{\rm sat}/M_{\rm host} > 0.3$.

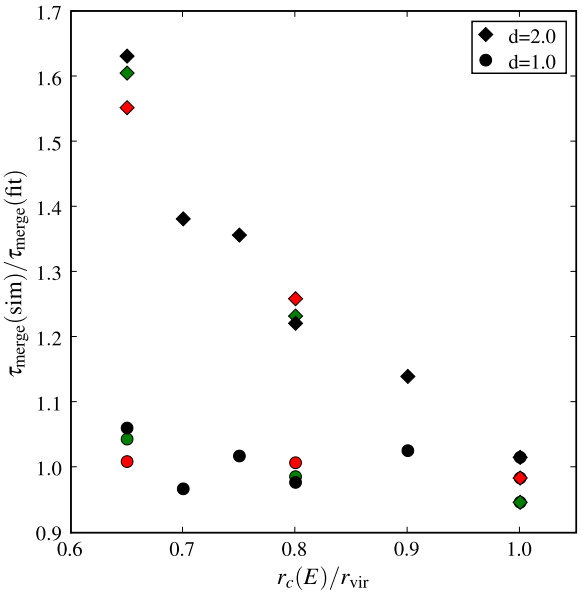

FIG. 3.— Comparison of merger time measured in our N-body simulations, $\tau_{\rm merge}$(sim), with the predicted $\tau_{\rm merge}$(fit) based on eq. (5), as a function of orbital energy $r_c(E)/r_{\rm vir}$. The orbital circularity is color-coded: $\eta = 0.33$ (red), 0.46 (green), and 0.65 (black). The circles use the best-fit parameters in eq. (6) and show the close agreement in $\tau_{\rm merge}$ between the simulations and the fits. The diamonds, on the other hand, illustrate the poor match when the energy dependence in eq. (5) is taken to be the conventional $d = 2.0$ instead of $d = 1.0$. All points are for $M_{\rm sat}/M_{\rm host} = 0.1$.

We have covered a range of circularities – $0.3 \le \eta \le 1.0$ – that includes the most likely values based on analyses of orbits in dark matter simulations ($\eta \approx 0.5$; e.g., Benson 2005; Zentner et al. 2005; Khochfar & Burkert 2006). Equation (5) should not be used for $\eta \lesssim 0.2$ because such orbits pass sufficiently close to the center of the host halo on their first pericentric passage that interaction with the central galaxy is important and will decrease the merging timescale.

The range of orbital energies considered here – $0.65 \le r_c(E)/r_{\rm vir} \le 1.0$ – also covers the peak values of distributions seen in cosmological simulations. We have limited ourselves to one specific scaling of dark matter halo scale radii – $a \propto M^{0.5}$ – that is motivated by analyses of cosmological N-body simulations (e.g., Bullock et al. 2001), which show that concentrations scale as $c \propto M^{-0.13}$. Taffoni et al. (2003) found that the dependence of $\tau_{\rm merge}$ on the satellite concentration is relatively weak: using their eq. 27, varying $c_{\rm sat}/c_{\rm host}$ between 1 and 2 results in a change in $\tau_{\rm merge}$ of only $\approx 20\%$.

3.3. *Comparison to Previous Work*

3.3.1. *Exponent b: dependence on mass ratio*

One important difference between equations (2) and (5) is the non-linear dependence on the mass ratio in equation (5). Our fitted value of $b = 1.3$ reflects an important difference between point masses and realistic dark matter satellites sinking in a larger host potential, as the dark matter halos continually lose mass

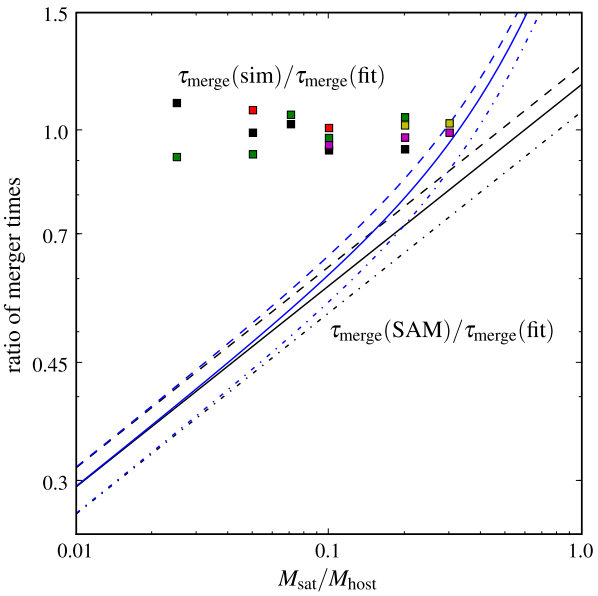

FIG. 4.— Comparison of merger times computed from N-body simulations, fitting formula eq. (5), and a fiducial SAM using eq. (2) and two choices of Coulomb logarithm (black and blue curves), for a variety of satellite-to-host mass ratios $M_{\rm sat}/M_{\rm host}$ and orbital circularities η, with $r_c(E)/r_{\rm vir} = 1$. The square symbols show the ratio $\tau_{\rm merge}({\rm sim})/\tau_{\rm merge}({\rm fit})$ and illustrate that the simulations and fit agree well, with an error of $\lesssim 10\%$. The orbital circularities are color-coded: $\eta = 0.33$ (red), 0.46 (green), 0.65 (black), 0.78 (magenta), and 1.0 (yellow). The fiducial SAM, on the other hand, generally underestimates the merging time, particularly at small $M_{\rm sat}/M_{\rm host}$, as shown by the three curves for different circularities: $\eta = 0.25$ (solid), 0.5 (dashed), and 0.75 (dot-dashed). The SAM here assumes $f_{df} = 1$, $\Theta_{\rm orb} = \eta^{0.78}$, and $r_c(E)/r_{\rm vir} = 1$. The different color curves correspond to different choices of Coulomb logarithms for the SAM: $\ln(1 + M_{\rm host}/M_{\rm sat})$ [black curves] and $\frac{1}{2}\ln(1 + M^2_{\rm host}/M^2_{\rm sat})$ [blue curves]

via tidal stripping and gravitational shocking against the host potential. The effective mass of the satellite over its lifetime is therefore smaller (sometimes substantially smaller) than its mass when entering the host halo. It is therefore not surprising that extended satellites sink more slowly than the standard formula predicts, leading to $b > 1$.

The exact exponent b turns out to be difficult to model from first principles as it depends on a number of factors. As an example, Fujii et al. (2006) and Fellhauer & Lin (2007) have shown that the effective mass (with regards to dynamical friction) of a sinking satellite is actually larger than the instantaneous bound mass because the mass that has been recently stripped also contributes to the drag force on the satellite. We see the same effect in our simulations, significantly complicating any effort to assume that either the bound mass or the instantaneous tidal mass is the relevant mass at every time.

3.3.2. *Parameters c and d: dependence on satellite orbits*

A common choice for the angular momentum dependence in equation (5) is $\tau_{\rm merge} \propto \eta^{0.78}$ (Somerville & Primack 1999; Cole et al. 2000), which Lacey & Cole (1993) found to be a good match to their integration of the orbit-averaged equations for energy and angular momentum loss for a point mass subhalo due to dynamical friction in an isothermal potential. van den Bosch et al. (1999) found a somewhat weaker angular momentum dependence in their numerical simulations (using point-mass satellites and an isothermal potential), $\tau_{\rm merge} \propto \eta^{0.53}$, while Taffoni et al. (2003) provide a more complex fitting formula for both point-mass and live satellites with realistic internal structure in an NFW potential.

We find that an exponential dependence – $\tau_{\rm merge} \propto \exp(c\,\eta)$ with $c = 1.9$ – provides a better fit to our simulations than a pure power law: a fit in which we force $\tau_{\rm merge} \propto \eta^{0.78}$ has a standard deviation of 14 % and a maximum deviation of 42% when compared to the simulations (compared to 6.7 % and 12 %, respectively, when using our fit). It is important to note, however, that it is the long $\tau_{\rm merge}$ for the $\eta = 0.78$ and $\eta = 1.0$ simulations that result in better agreement using the exponential fit rather than the power-law fit. If we restrict our attention to runs with $0.33 \leq \eta \leq 0.65$, we find that $\tau_{\rm merge} \propto \eta^{0.78}$ does indeed provide a good fit to our simulation results.

Our revised fitting formula has a somewhat weaker dependence on η for $\eta \lesssim 0.5$ and a stronger dependence for $\eta \gtrsim 0.5$ relative to that found by previous work with point-mass satellites. Both of these limits are plausible: for small η (nearly radial orbits), a slight change in η should have a negligible effect on $\tau_{\rm merge}$ since the orbits will have small pericentric distances. For large η (nearly circular orbits), live satellites still lose mass at large radii, reducing their mass and lengthening their $\tau_{\rm merge}$ relative to an equivalent point-mass satellite. The same is true for live satellites on more radial orbits but to a lesser degree, as angular momentum losses correlate well with pericentric passages (see Fig. 1); the net effect creates a stronger dependence on η for $\eta \gtrsim 0.6$ for live satellites than for point-mass satellites.

For the orbital energy dependence of the merger timescale, we find that $d = 1.0$ is the best fit to our simulations. This is to be contrasted with the canonical value of $d \approx 2.0$ in prior work. The latter is appropriate for an isothermal host (e.g., eq. 7.26 of Binney & Tremaine 1987), or for *point mass* satellites sinking on circular orbits in a static potential, as can be determined by integrating equation (1). This yields $\tau_{\rm merge} \propto (r_c(E)/r_{\rm vir})^{1.97}$ for an NFW potential (Taffoni et al. 2003). We find that for point-mass satellites on circular orbits in a host halo with a Hernquist density profile and scale radius a, the energy dependence of $\tau_{\rm merge}$ has an analytic expression,

$$\tau_{\rm merge} \propto \sqrt{x}\left(\frac{1}{10}\,x^2 + \frac{1}{3}\,x - 1 + \frac{\tan^{-1}\sqrt{x}}{\sqrt{x}}\right), \qquad (7)$$

where $x \equiv r_c(E)/a$. Equation (7) can be well-approximated by $\tau_{\rm merge} \propto r_c(E)^{2.3}$ for $0.2 \leq x \leq 30$, comparable to $d = 2$. The difference between these results for point masses and our best-fit value of $d = 1$ lies in our study of live satellites and in our definition of $M_{\rm sat}$. Because of ambiguities in defining $M_{\rm sat}$ at small radii when significant tidal stripping has occurred, we have chosen to use virial quantities exclusively in equation (5), including for the satellite mass $M_{\rm sat}$. Were we to use *locally*-defined quantities such as $M_{\rm sat}(t)$, we would expect that $M_{\rm sat}(t) \propto r(t)$ for an isothermal sphere, so that the merger time evaluated as a function of radius is given by $\tau_{\rm merge} \propto r^2(t)/M_{\rm sat}(t) \propto r(t)$. It is therefore not surprising that we find $d \sim 1$ to be a better match

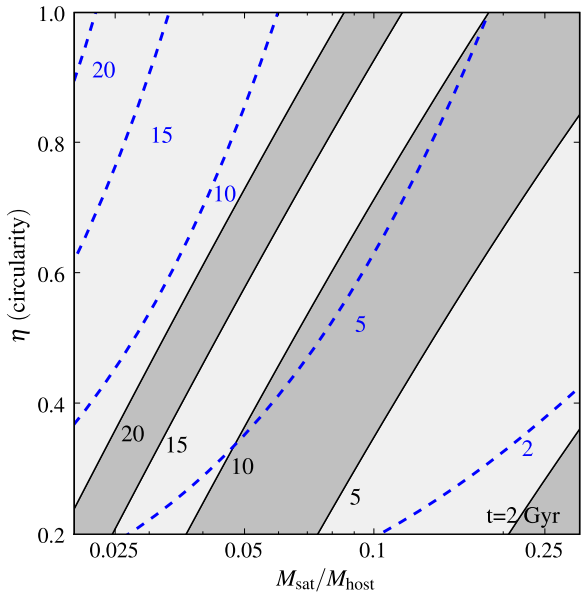

FIG. 5.— Contours of equal τ_{merge} in the space of satellite-to-host mass ratio M_{sat}/M_{host} and orbital circularity η, assuming $r_c(E) = r_{vir}$. The black solid curves represent our fitting formula eqs. (5) and (6); the blue dashed curves correspond to the same SAM shown in Fig. 4. The labelled times are for a host halo with $M_{host} = 10^{12}\,M_\odot$ and $a = 40$ kpc. The SAM generally underpredicts τ_{merge}, with the largest discrepancy at large η and small M_{sat}/M_{host}.

than $d \approx 2$ to our numerical results.

3.3.3. *Numerical comparison*

In Figs. 4 and 5 we quantify the differences between equation (5) and prior work discussed in the previous two subsections. Fig. 4 compares τ_{merge}(SAM) from a fiducial SAM using equation (2) and τ_{merge}(fit) from our fits to equation (5) for a range of satellite-to-host mass ratio M_{sat}/M_{host} and orbital circularity ($\eta = 0.25$, 0.5, and 0.75 for the solid, dashed and dot-dashed curves, respectively). The SAM here assumes $f_{df} = 1$, $\Theta_{orb} = \eta^{0.78}$, and $\ln\Lambda = \ln(1+M_{host}/M_{sat})$. The curves illustrate that the fiducial SAM *underestimates* the merger timescale at all masses we have considered regardless of the orbital circularity. Moreover, the disagreement grows as the satellite mass decreases relative to the host: at $M_{sat}/M_{host} = 0.2$ the SAM timescale is too small by approximately 50%, while the discrepancy increases to a factor of 3 at $M_{sat}/M_{host} = 0.025$. If a Coulomb logarithm of $\Lambda = 1 + (M_{host}/M_{sat})^2$ is used (Somerville & Primack 1999), the discrepancy increases further by approximately a factor of 2 for $M_{sat} \ll M_{host}$. In order to provide a better match to simulations or observations, some groups adjust the normalization of τ_{merge} by setting $f_{df} \neq 1$ (e.g., de Lucia & Blaizot 2007, $f_{df} = 2$; Bower et al. 2006, $f_{df} = 1.5$; and Nagashima et al. 2005, $f_{df} = 0.8$). Although $f_{df} > 1$ goes in the right direction, Figure 4 shows that a constant f_{df} does a poor job of matching the numerical results.

Fig. 5 compares the contours of constant τ_{merge} in the space of mass ratio M_{sat}/M_{host} and orbital circularity η, as predicted from our fits in equation (5) (solid curves) and the same SAM from Fig. 4 (dashed curves). The two sets of curves are for the same five merger times: 2, 5, 10, 15, and 20 Gyr. All orbits that lie to the right of and below a given contour will merge within the time corresponding to that contour, while those to the left of and above a contour will not. Fig. 5 shows that even the predictions for orbits with the fastest merging times – those with low circularities and large mass ratios (the lower-right portion of the figure) – differ between the SAM and our fit. At larger circularities or smaller mass ratios, the two predictions deviate significantly. As an example, the prediction from our revised formula for 20 Gyr merging times is similar to the curve for 10 Gyr merging times in the SAM.

Our results can be compared to the fitting formulae provided by Taffoni et al. (2003) [and updated by Monaco et al. 2007], which are valid for $0.3 \leq r_c(E)/r_{vir} \leq 0.9$. The overall trend we find is qualitatively similar to the results of Taffoni et al. (e.g., their Fig. 7), but the quantitative details are somewhat different. We find that massive satellites ($M_{sat}/M_{host} \gtrsim 0.05$) sink more slowly than predicted by Taffoni et al. while light satellites sink more quickly. For example, we predict a timescale that is 25% shorter than Taffoni et al. for $M_{sat}/M_{host} = 0.025$, $r_c(E)/r_{vir} = 0.75$, and $\eta = 0.65$ but find a timescale that is 40% longer for a satellite with $M_{sat}/M_{host} = 0.1$ and identical orbital parameters. Fig. 7 of Taffoni et al. also shows that the deviation of live satellite merger times from a fiducial SAM prediction is not monotonic with M_{sat}/M_{host} as is suggested by our Fig. 4 and equation (5). In particular, for $M_{sat}/M_{host} \lesssim 0.001$ and $M_{sat}/M_{host} \gtrsim 0.2$, τ_{merge} is approximately the same in the extended and point mass cases. We have not explored mass ratios lower than 1:100, however, because the sinking times exceed many Hubble times.

After this paper was submitted, Jiang et al. (2007, hereafter J07) independently investigated the merging timescales of satellites using N-body simulations and came to a similar overall conclusion as that in this paper, namely, that Eqn. 2 generally underpredicts merging timescales. J07 used a different N-body approach – cosmological simulations including hydrodynamics – and obtained a fitting formula that differs in its details from ours. Specifically, J07 found $b = 1$ (rather than 1.3) and a significantly weaker dependence on circularity. The aforementioned differences between the methods used in this study and J07, as well as differences in definitions (e.g., we define halo radii relative to $200\,\rho_c$ while J07 use $\Delta_v(z)\,\rho_c$) make a direct comparison non-trivial. However, even for our most major mergers ($M_{sat}/M_{host} \geq 0.1$, runs 3x, 5x, and 10x), we still find a significantly stronger dependence on η than J07: whereas the fitting formula in J07 predicts a difference in τ_{merge} of only 30% between $\eta = 0.46$ and $\eta = 1$ orbits, we find a difference of 160% (runs 5b and 5e). In addition, we find that at fixed orbital parameters, the difference in merger times between our most major merger simulations (the 0.3:1 and 1:5 runs) is somewhat better fit by $b = 1$ than $b = 1.3$. Most of the non-linear dependence on mass-ratio that we find in equation 6 is thus due to the larger mass ratio (more minor) mergers. This suggests that the difference between our preferred value of $b = 1.3$ and J07's value of $b = 1$ may be due to the range of mass ratios considered.

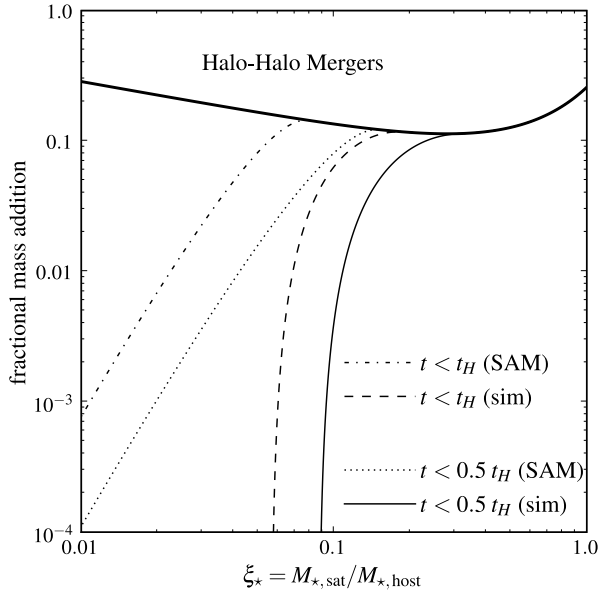

FIG. 6.— Fraction of stellar mass gained through mergers (i.e., satellite accretion) at the host's virial radius $r_{\rm vir}$ that makes it down to the central galaxy in time t, as a function of the satellite-to-host stellar mass ratio $\xi_\star$. The thick solid line is the number of halo-halo mergers at $r_{\rm vir}$ as a function of mass ratio $\xi_\star$ (normalized to integrate to unity). We consider the predictions of both the fiducial SAM from Fig. 4 and our eqn. (5). The fiducial SAM predicts that approximately 40% more mass is accreted in one Hubble time, all of which is in low-$\xi_\star$ mergers.

4. A SAMPLE APPLICATION

The merger timescale given by equation (5) can be applied to a wide variety of astrophysical problems. We defer most of these to future papers. To give one concrete example, however, we briefly consider the dissipationless growth of stellar mass for galaxies at the centers of dark matter halos.

In a finite time period, whether or not galaxies can merge following the merger of their much more extended host halos depends on $\tau_{\rm merge}$ due to dynamical friction. Given the dark matter halo-halo merger rate $\mathrm{d}^2N_m/\mathrm{d}\xi\mathrm{d}z$ at some redshift z, defined as the average number of mergers with mass ratio $\xi = M_2/M_1 \leq 1$ leading to halos of mass $M = M_1 + M_2$ per halo per redshift per ξ, the corresponding growth of stellar mass over a time interval t can be computed using

$$\frac{\mathrm{d}^4M_\star}{\mathrm{d}\xi\,\mathrm{d}\eta\,\mathrm{d}E\,\mathrm{d}z} = M_\star(M_2)\frac{\mathrm{d}^2N_m}{\mathrm{d}\xi\,\mathrm{d}z}\frac{\mathrm{d}^2P}{\mathrm{d}\eta\,\mathrm{d}E}\,\Theta(t-\tau_{\rm merge}) \quad (8)$$

where $\mathrm{d}^2P/\mathrm{d}\eta\,\mathrm{d}E$ is the probability of two dark matter halos merging with orbital circularity η and energy E (typically measured when the two halos' virial radii touch), Θ is the unit step function, and $M_\star(M_2)$ is the stellar mass as a function of dark matter mass. The step function in equation (8) enforces the fact that only galaxies in halos with $\tau_{\rm merge} \leq t$ can merge with the central host galaxy in time t. A full calculation of $\mathrm{d}M_\star/\mathrm{d}t$ would require an appropriate integral of equation (8) over time t, so that all halo-halo mergers are accounted for. Results of the full calculation will be presented in Boylan-Kolchin et al. (in preparation); here we consider instead the simpler problem of using equation (8) to calculate the fraction of the stellar mass accreted at redshift z at $r_{\rm vir}$ that makes it down to the center within time t. In particular, by integrating equation (8), the stellar mass accreted in satellites of different mass, circularity, or energy can be computed.

We first consider the mass spectrum of merging objects that determines whether most of the stellar mass added to the galaxy comes from a small number of massive progenitors or a large number of low-mass progenitors. This is obtained from equation (8) by integrating over η and E, taking into account the dependence of $\tau_{\rm merge}$ on each of these orbital parameters. Zentner et al. (2005) found that $\mathrm{d}P/\mathrm{d}\eta \propto \eta^{1.2}\,(1-\eta)^{1.2}$, which we use in equation (8). For simplicity, we assume that all orbits have an energy equal to the energy of a circular orbit at the host's virial radius ($r_c(E) = r_{\rm vir}$), i.e., $\mathrm{d}P/\mathrm{d}E = \delta[E - E_c(r_{\rm vir})]$. The halo merger rate is taken from the analysis of Fakhouri & Ma (2007, in preparation), who have analyzed merger rates in the Millennium simulation (Springel et al. 2005b) and find that

$$\frac{\mathrm{d}^2N_m}{\mathrm{d}\xi\,\mathrm{d}z} \propto \xi^{-1.92}\,\exp\left[\left(\frac{\xi}{0.125}\right)^{0.4}\right]. \quad (9)$$

Finally, we assume that dark matter halo mass and the stellar mass of its central galaxy scale as $M_{dm} \propto M_\star^{1.5}$, which is appropriate for massive galaxies in groups and clusters (Guzik & Seljak 2002; Hoekstra et al. 2005; Mandelbaum et al. 2006).

Fig. 6 shows how different dynamical friction prescriptions lead to different cutoffs at the low mass end for the fraction of mass assembled via mergers of a given (stellar) mass ratio $\xi_\star$. We plot both the predictions of our numerical fit in equation (5) and the fiducial SAM from Fig. 4. Techincally, we should consider orbits with $\eta \lesssim 0.2$ separately from those with $\eta \gtrsim 0.2$, as the dynamics of very radial mergers can be strongly affected by the stellar components of the merging galaxies at first pericentric passage, introducing complications that we have not considered in our current analysis. For illustrative purposes, however, these orbits, which account for $\approx 9\%$ of the accreted mass at $r_{\rm vir}$, are included in Fig. 6.

In all of the calculations in Fig. 6, a wide range of $\xi_\star \sim 0.1-1$ contribute to the mass growth of the central galaxy. For a canonical SAM dynamical friction formula, however, a non-negligible amount of extra mass is added in low mass ratio mergers, relative to the predictions of our formula for $\tau_{\rm merge}$. In fact, $\mathrm{d}M_\star/\mathrm{d}t$ is approximately 40% larger for $t = t_H$ for the canonical SAM formula for $\tau_{\rm merge}$, and all of the extra mass is accreted in low-ξ mergers.

Dynamical friction also distorts the orbital distribution of satellites at $r_{\rm vir}$ of the host, preferentially selecting low angular momentum orbits for accretion onto the central galaxy. This effect is shown in Fig. 7, which shows the initial distribution of orbital circularities (dashed curve; taken from Zentner et al. and assumed to be independent of ξ) along with the distribution of circularities for satellites merging within a given fraction of a Hubble time ($\tau_{\rm merge}/t_H = 0.1$, 0.316, 1.0, and 3.16). For $\tau_{\rm merge}/t_H \gg 1$, the stellar mass accreted as a function of circularity should approach the circularity distribution at $r_{\rm vir}$, as all satellites will eventually merge. As $\tau_{\rm merge}/t_H$ decreases, however, the peak of the distribution shifts to

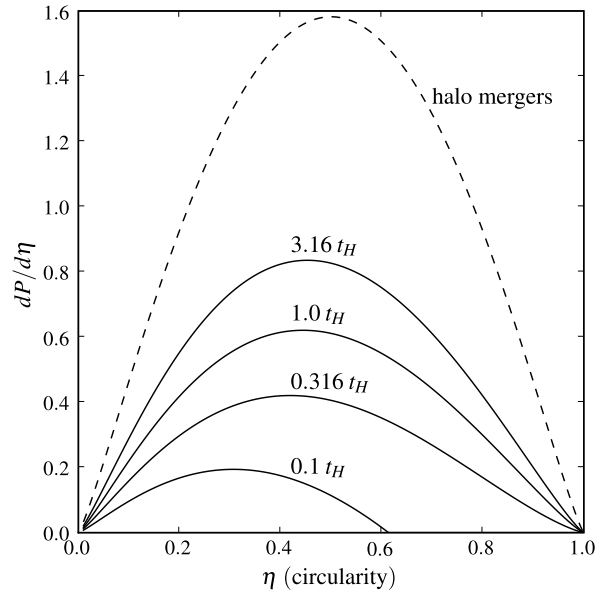

FIG. 7.— Impact of dynamical friction on the orbital properties of satellites that merge with a central galaxy. The input distribution of circularities η for halo-halo mergers at $r_{\rm vir}$ with $\xi > 10^{-3}$ is shown with the dashed curve ($dP/d\eta$, taken from Zentner et al. 2005). The solid curves show the predicted distribution of η for satellite galaxies that merge onto the central galaxy within a specific fraction of a Hubble time using equation (5). Higher mass ratio and lower angular momentum orbits preferentially accrete, leading to a shift in the $dP/d\eta$ distribution to lower circularities.

smaller and smaller circularities because low angular momentum satellites merge more rapidly. Fig. 7 shows that the peak of the input distribution of circularities ($\mathrm{d}P/\mathrm{d}\eta$) is at $\eta = 0.5$ but that most of the mass comes in via satellites on orbits with $\eta = 0.42$ at $\tau_{\rm merge}/t_H = 1$ and with $\eta = 0.30$ for $\tau_{\rm merge}/t_H = 0.1$. Shifting the peak of the circularity distribution from 0.5 to 0.42 corresponds to a 30% reduction in the pericentric distance of the orbit, which can have a significant effect on the properties of the merger remnant (see, e.g., Boylan-Kolchin et al. 2006).

5. CONCLUSIONS

Applications of dynamical friction to problems in galaxy formation are often based on classic results derived for point masses sinking in a galaxy with an isothermal density profile (e.g., eq. [2]). Using direct numerical simulations, we have shown that live dark matter satellites with realistic internal structure and mass ratios in the range relevant for galaxy formation ($0.02 \lesssim M_{\rm sat}/M_{\rm host} \lesssim 0.3$) take much longer to merge than the corresponding point-mass satellite results, which are typically used in semi-analytic galaxy formation models (e.g., Figs. 3-5). This difference is primarily because the satellites undergo significant mass loss as they sink deeper in the potential well of the host halo. Including a stellar bulge in both the satellite and host changes the merger time by $\lesssim 10\%$ for typical orbital circularities (see Fig. 2). We find that the surprisingly simple fitting formula given in equations (5) and (6) provides an accurate ($\lesssim 10\%$ error) fit to the numerically determined galaxy merging times over the range of mass ratios, orbital circularities, and orbital energies we have considered. The dependence of $\tau_{\rm merge}$ on mass ratio, energy, and angular momentum implied by this fit is all somewhat different from standard assumptions in the literature (see §3.3). We have chosen to test our results for a range of parameters that are cosmologically interesting, e.g. for satellite-to-host mass ratios for which the satellite undergoes significant orbital evolution within a Hubble time, and for orbital parameters that are relvant according to cosmological dark matter simulations.

The results of this paper should be relevant to a wide range of problems in galaxy formation and evolution. For example, halo-halo merger rates as a function of mass ratio $M_{\rm sat}/M_{\rm host}$ from extended Press-Schechter theory or cosmological simulations show that a significant amount of dark matter mass is accumulated via accretion of lower-mass halos with $0.02 \lesssim M_{\rm sat}/M_{\rm host} \lesssim 0.3$ (e.g., eq. [9] & Fig. 6; Lacey & Cole 1993; Zentner 2007; Fakhouri & Ma 2007, in prep). Understanding the evolution of the galaxy population in such halos thus requires an accurate understanding of the effects of dynamical friction in precisely the mass range where the point mass approximation is inadequate. To give a few concrete examples, we have shown that standard merging timescales in the literature overestimate the growth of stellar mass by satellite accretion by $\approx 40\%$, with the extra mass gained in low mass ratio mergers (Fig. 6). In addition, we have quantified the tendency for satellites that accrete onto a central galaxy to have lower angular momentum than average: the peak in the circularity distribution shifts from ≈ 0.5 to ≈ 0.42 when one considers only satellites that merge onto a central galaxy within a Hubble time (Fig. 7).

Several limitations of our calculations should be noted. For orbits with very low circularity ($\eta \lesssim 0.2$), our results are not applicable because such orbits pass sufficiently close to the center of the host halo on their first pericentric passage that interaction with the central galaxy is important and will decrease the merging timescale. All but two of our 28 simulations neglect the effect of the central galaxy in a given dark matter halo on the merging timescale. As Fig. 2 shows, this is a reasonable approximation when considering merging from the virial radius (as we have done), but would be less applicable for studying the detailed evolution of satellites at small radii in a dark matter halo (e.g. Ostriker & Hausman 1977). Finally, our results do not take into account drag on ambient gas, which may be important in cluster and group environments (e.g., Ostriker 1999).

We thank the referee for useful suggestions and Volker Springel for making GADGET-2 publicly available. This work used resources from NERSC, which is supported by the US Department of Energy. C-PM is supported in part by NSF grant AST 0407351. EQ is supported in part by NASA grant NNG05GO22H and the David and Lucile Packard Foundation.

REFERENCES

Benson, A. J. 2005, MNRAS, 358, 551
Binney, J., & Tremaine, S. 1987, Galactic Dynamics (Princeton, NJ, Princeton University Press)
Bower, R. G., Benson, A. J., Malbon, R., Helly, J. C., Frenk, C. S., Baugh, C. M., Cole, S., & Lacey, C. G. 2006, MNRAS, 370, 645
Boylan-Kolchin, M., & Ma, C.-P. 2007, MNRAS, 374, 1227
Boylan-Kolchin, M., Ma, C.-P., & Quataert, E. 2006, MNRAS, 369, 1081
Bullock, J. S., Kolatt, T. S., Sigad, Y., Somerville, R. S., Kravtsov, A. V., Klypin, A. A., Primack, J. R., & Dekel, A. 2001, MNRAS, 321, 559
Chandrasekhar, S. 1943, ApJ, 97, 255
Cole, S., Lacey, C. G., Baugh, C. M., & Frenk, C. S. 2000, MNRAS, 319, 168
Cooray, A., & Milosavljević, M. 2005, ApJ, 627, L85
Croton, D. J. et al. 2006, MNRAS, 365, 11
de Lucia, G., & Blaizot, J. 2007, MNRAS, 375, 2
Fellhauer, M., & Lin, D. N. C. 2007, MNRAS, 375, 604
Fujii, M., Funato, Y., & Makino, J. 2006, PASJ, 58, 743
Gnedin, O. Y. 2003, ApJ, 589, 752
Guzik, J., & Seljak, U. 2002, MNRAS, 335, 311
Hashimoto, Y., Funato, Y., & Makino, J. 2003, ApJ, 582, 196
Hernquist, L. 1990, ApJ, 356, 359
Hoekstra, H., Hsieh, B. C., Yee, H. K. C., Lin, H., & Gladders, M. D. 2005, ApJ, 635, 73
Jiang, C. Y., Jing, Y. P., Faltenbacher, A., Lin, W. P., & Li, C. 2007, arXiv:0707.2628 [astro-ph]
Kauffmann, G., White, S. D. M., & Guiderdoni, B. 1993, MNRAS, 264, 201
Khochfar, S., & Burkert, A. 2006, A&A, 445, 403
Lacey, C., & Cole, S. 1993, MNRAS, 262, 627
Mandelbaum, R., Seljak, U., Kauffmann, G., Hirata, C. M., & Brinkmann, J. 2006, MNRAS, 368, 715
Monaco, P., Fontanot, F., & Taffoni, G. 2007, MNRAS, 375, 1189
Nagashima, M., Yahagi, H., Enoki, M., Yoshii, Y., & Gouda, N. 2005, ApJ, 634, 26
Navarro, J. F., Frenk, C. S., & White, S. D. M. 1997, ApJ, 490, 493
Ostriker, E. C. 1999, ApJ, 513, 252
Ostriker, J. P., & Hausman, M. A. 1977, ApJ, 217, L125
Shen, S., Mo, H. J., White, S. D. M., Blanton, M. R., Kauffmann, G., Voges, W., Brinkmann, J., & Csabai, I. 2003, MNRAS, 343, 978
Somerville, R. S., & Primack, J. R. 1999, MNRAS, 310, 1087
Springel, V. 2005, MNRAS, 364, 1105
Springel, V., Di Matteo, T., & Hernquist, L. 2005a, MNRAS, 361, 776
Springel, V. et al. 2005b, Nature, 435, 629
Taffoni, G., Mayer, L., Colpi, M., & Governato, F. 2003, MNRAS, 341, 434
Taylor, J. E., & Babul, A. 2001, ApJ, 559, 716
van den Bosch, F. C., Lewis, G. F., Lake, G., & Stadel, J. 1999, ApJ, 515, 50
Velazquez, H., & White, S. D. M. 1999, MNRAS, 304, 254
White, S. D. M. 1976, MNRAS, 174, 467
York, D. G. et al. 2000, AJ, 120, 1579
Zentner, A. R. 2007, International Journal of Modern Physics D, 16, 763
Zentner, A. R., Berlind, A. A., Bullock, J. S., Kravtsov, A. V., & Wechsler, R. H. 2005, ApJ, 624, 505